Dalton
Transactions

Cite this: *Dalton Trans.*, 2012, **41**, 9753

www.rsc.org/dalton

PAPER

Tri-, hepta- and octa-nuclear Ag(I) complexes derived from 2-pyridyl-functionalized tris(amido)phosphate ligand†

Arvind K. Gupta,[a] Alexander Steiner[b] and Ramamoorthy Boomishankar*[a]

Received 2nd February 2012, Accepted 31st May 2012
DOI: 10.1039/c2dt30241a

Mild deprotonation of a 2-pyridyl (py)-functionalized phosphoric triamide [PO(NHpy)$_3$] in the absence of an external base was studied in the presence of various silver(I) salts. Interesting examples of octa- and hepta-nuclear Ag(I) complexes coordinated to imido and pyridyl groups were obtained when more reactive Ag(I) salts, such as $AgClO_4$ and $AgBF_4$, were used, while the less reactive $AgNO_3$ reacts only with the peripheral pyridyl groups leading to a tri-nuclear cluster. Structural determination of these Ag(I) complexes show that sequential deprotonation of the ligand amino protons were achieved forming imido P(V) species analogous to the $H_2PO_4^-$ and HPO_4^{2-} ions.

Introduction

Polyimido anions of the main group elements have been a topic of interest for several research groups.[1] These are isoelectronic analogues of the common oxo anions and have been utilized as ligands in coordination chemistry.[2] In this context, phosphorus-bound imido anions have received considerable attention.[3] For example, the homoleptic imido analogues of the respective P(V) oxo species H_3PO_4, $H_2PO_4^-$, HPO_4^{2-} and PO_4^{3-} have been obtained by the sequential deprotonation of the phosphonium cation $[(PhNH)_4P]^+$ by *n*-butyllithium.[4] Chivers and coworkers have shown that tris(organoamino) phosphates of formula $(RNH)_3P{=}E$ (E = NR′, O, S or Se) can be deprotonated with a wide variety of organometallic bases, such as RLi, R_2Zn, R_2Mg and R_3Al (R is any alkyl or aryl group), generating interesting examples of imido phosphate anions (Fig. 1). Formation of multi-nuclear metal complexes have been envisaged in many of these reactions, wherein the steric bulk on the imido ligands and nature of the metal ions plays a vital role in controlling their degree of oligomerization.[5,6] Oxidation of some of these metal complexes has been shown to form long-lived paramagnetic radicals.[7] In addition, metal complexes of several iminophosphoranes were implicated as catalytic systems for olefin oligomerization[8] and polymerization,[9] ring-opening polymerization of lactides,[10] hydroamination[11] and transfer hydrogenation[12] reactions. Previously, our group has been involved in synthesizing phosphonium cations of the formula $[(RNH)_4P]^+$, in the presence of chloride, carboxylate and polyoxometalate anions, in making designer supramolecular structures aided by hydrogen bonding interactions.[13] In view of the versatile coordination abilities of the imino moiety, we were interested in looking at imido P(V) ligands containing peripheral functional groups and utilizing them for obtaining multi-metallic assemblies. In this effort, we recently synthesized a tetra 2-pyridyl (py)-attached phosphine imine [P(Npy)(NHpy)$_3$] starting from the phosphonium salt [P(NHpy)$_4$]Cl and showed that both of them undergo deprotonation in presence of a silver salt ($AgClO_4$), yielding the homoleptic imido-phosphinate ion $[P(Npy)_2(NHpy)_2]^-$ ($L^1H_2^-$) as a penta-nuclear $[Ag_5(L^1H_2)_2]^{3+}$ complex.[14] In this paper, we report on the synthesis of two imido P(V) species analogous to the dihydrogen phosphate $[PO(Npy)(NHpy)_2]^-$ (LH_2^-) and mono hydrogen phosphate $[PO(Npy)_2(NHpy)]^{2-}$ (LH^{2-}) ions, as their octa-nuclear $[Ag_8(LH_2)_4]^{4+}$ (**3**) and hepta-nuclear $[Ag_7(LH)_3]^+$ (**4**) complexes, respectively. These anions were generated *in situ* in the reactions involving [PO(NHpy)$_3$] (**1**) and the Ag(I) salts containing (ClO_4^-) and (BF_4^-) anions. We also observed the formation of a tri-nuclear $[Ag_3(LH_3)_2]^{3+}$ complex **2** in the reaction of **1** with $AgNO_3$ where phosphoric triamide **1** acts as a neutral (LH_3) ligand.

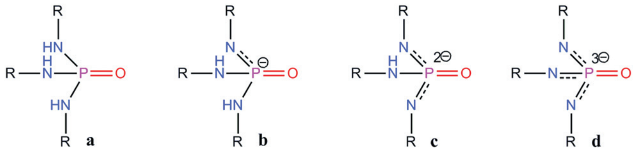

Fig. 1 N-analogues of various P(V) oxo anions.

---

[a] *Department of Chemistry, Mendeleev Block, Indian Institute of Science Education and Research (IISER), Pune, Dr. Homi Bhabha Road, Pune 411008, India. E-mail: boomi@iiserpune.ac.in; Fax: +91 2025908186*
[b] *Department of Chemistry, University of Liverpool, Crown Street, Liverpool L69 7ZD, United Kingdom*

† Electronic supplementary information (ESI) available: Selected bond-lengths and angles, H-bonding table, ^{31}P-NMR spectra, PXRD patterns and addtional figures. CCDC 865262–865265 and 882870 for **1**·C_7H_8, **2**, **3** and **4**. For ESI and crystallogrphic data in CIF or other electronic format see DOI: 10.1039/c2dt30241a

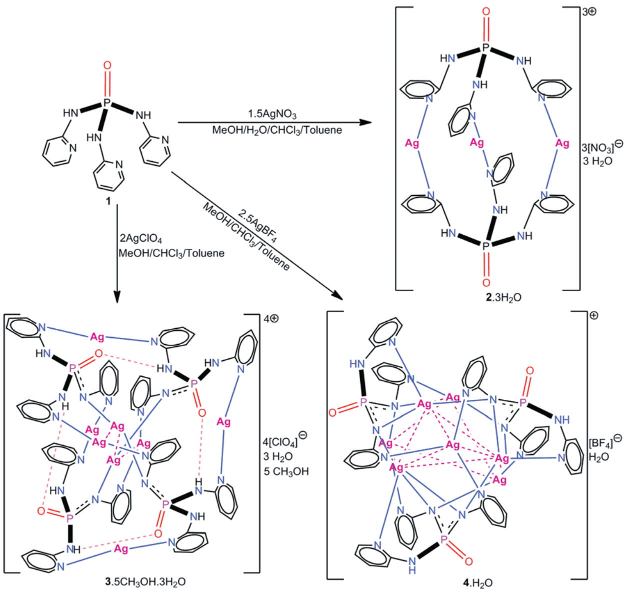

Scheme 1 Reaction conditions for the preparation of the Ag(I) clusters.

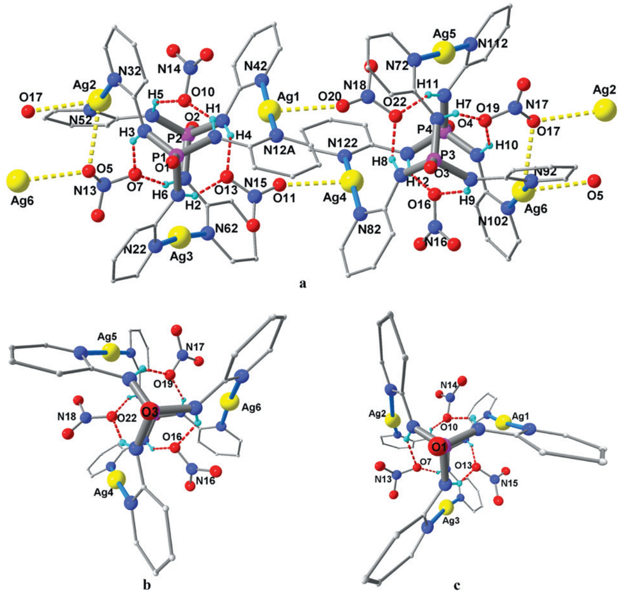

Fig. 2 (a) The molecular structure of $\mathbf{2}\cdot 3H_2O$ showing the interaction between the two tri-cationic motifs. Solvated water molecules have been omitted for clarity. The central projection of the anti-clockwise (b) and clockwise (c) rotation of the ligand arms in $\mathbf{2}\cdot 3H_2O$.

Results and discussion

Synthesis

The precursor ligand **1**, [PO(NHpy)$_3$], was synthesized according to our previously reported procedure, which involves the reaction of $POCl_3$ with an excess of 2-aminopyridine in refluxing toluene.[14] Spurred on by our earlier observation on the formation of a homoleptic [P(Npy)$_2$(NHpy)$_2$]$^-$ ion, we set out to test the mild deprotonation of **1** in the presence of various Ag(I) salts. Accordingly, **1** was treated separately with an excess of AgOAc, $AgNO_3$, $AgClO_4$, $AgBF_4$, $AgPF_6$, AgOTf and $AgSbF_6$ under similar reaction conditions. Typically, the reaction procedure involves the slow diffusion of a solution of the Ag(I) salt in methanol (methanol–water mixture in the cases of AgOAc and $AgNO_3$) to a solution of **1** in a methanol–chloroform–toluene mixture. Crystalline products were obtained in three instances where formation of $\mathbf{2}\cdot 3H_2O$, $\mathbf{3}\cdot 5CH_3OH\cdot 3H_2O$ and $\mathbf{4}\cdot H_2O$ as colourless crystals was observed within two weeks (Scheme 1). The single crystal X-ray analysis showed the mono- and di-anions of the type *b* and *c* (Fig. 1) were formed in the reactions involving $AgClO_4$ and $AgBF_4$ salts, respectively. Whereas, deprotonation of the ligand protons was not observed in the structure of **2** obtained in the reaction of **1** with $AgNO_3$. The ^{31}P-NMR (in d_6-DMSO) spectra of the metal complexes **2** (δ −5.2), **3** (δ +1.5) and **4** (δ +9.3) are progressively shifted downfield and closely match the literature reported values for the similar amido and imido P(V) species. The ^{31}P-CP-MAS NMR of the crystalline samples of **2**, **3** and **4** show less pronounced shifts than the solution spectra and give single peaks centred at δ −2.08, −1.78 and −0.95, respectively (Fig. S1, ESI†). In order to understand the preferential formation of mono and di-anions (LH_2^- and LH^{2-}) in reactions of Ag(I) salts, we separately treated **1** (0.031 mmol) with an excess of $AgClO_4$ (0.280 mmol) and $AgBF_4$ (0.298 mmol) in d_6-DMSO (2 mL) under stirring conditions. The ^{31}P-NMR of the reaction mixture in each of these reactions after three days showed two peaks at δ +9.3 and +1.5 (in addition to the free ligand peak at δ −4.9) indicating the presence of both [PO(Npy)(NHpy)$_2$]$^-$ and [PO(Npy)$_2$(NHpy)]$^{2-}$ ions, albeit in different ratios (Fig. S2, ESI†). These observations point to the fact that both anionic species were formed in solution in the reactions involving **1** and $AgClO_4$ or $AgBF_4$. The ESI-MS studies of the crystalline samples of **2**, **3** and **4** in methanol provided confirmation of the presence of the parent clusters in solution (Fig. S3, ESI†). Thus, for **2** and **4**, we observed peaks at *m*/*z* 972.9 and 1726.5, corresponding to the species $[Ag_3(LH_3)_2]^{3+}$ and $[Ag_7(LH)_3]^+$, respectively. Similarly for **3**, a series of peaks at *m*/*z* 540.9, 759.1 and 1186.7 were observed, corresponding to $\{[Ag_8(LH_2)_4](ClO_4)_{4-n}\}^{n+}$ ions (n = 4, 3, 2). In all of these cases, a major peak at *m*/*z* 433.0 was observed matching the smallest fragment $[Ag(LH_3)]^+$. In addition, signals corresponding to several prominent fragment ions, with different Ag to ligand ratios, were found in all of these spectra.

Crystal structures

The compound $\mathbf{2}\cdot 3H_2O$ crystallized in the chiral monoclinic space group $P2_1$. The asymmetric unit consists of two crystallographically independent tri-cationic cluster cores, six nitrate anions and six molecules of water. The Ag(I) cations in $\mathbf{2}\cdot 3H_2O$ are found in a two-coordinate environment and are bonded to pyridyl nitrogens from two different ligands (Fig. 2a). The Ag–N distances in $\mathbf{2}\cdot 3H_2O$ range from 2.14(2) to 2.203(17) Å, and the N–Ag–N angles are between 168.0(6) and 177.4(8)°. The cationic motif can be viewed as a trigonal bipyramidal cage structure, in which the three Ag(I) centres form the equatorial plane and the two P-atoms take up the axial sites. The average Ag–Ag separation within the cluster is 6.050 (3) Å, closely matching other $[Ag_3L_2]^{3+}$ cages containing relatively bulky tripodal ligands.[15] Each $[Ag_3(LH_3)_2]^{3+}$ unit in $\mathbf{2}\cdot 3H_2O$ offers

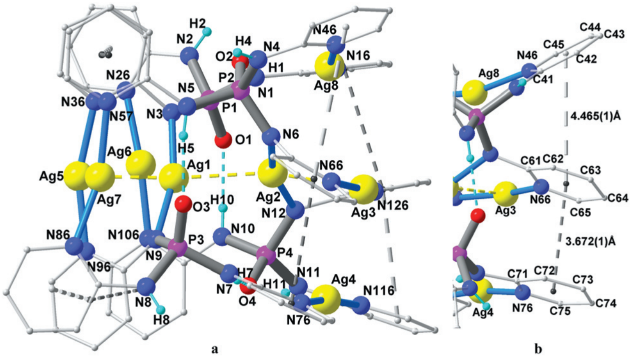

Fig. 3 (a) A view of the octa-nuclear cluster in **3**·$5CH_3OH·3H_2O$; (b) a closer view of one of the four π–π stacked triads.

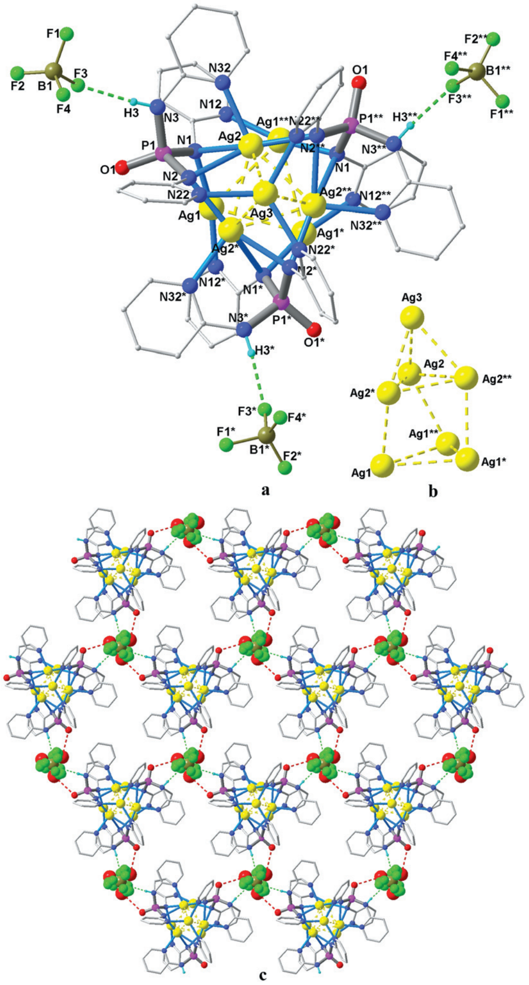

Fig. 4 (a) The molecular structure of the hepta-nuclear cluster in **4**·H_2O; (b) an inner view of the Ag_7 core; (c) formation of a 2D-hexagonal sheet structure aided by H-bonding interactions.

suitable binding pockets for three nitrate anions, which are held closer to the cationic cluster *via* H-bonding interactions with the amino protons. Furthermore, two of the three Ag(I) ions in each tri-cationic cluster make long contacts with the nitrate oxygens (av. Ag–O distance: 2.706(2) Å) that are housed at the adjacent cluster unit leading to a 1D-chain structure. While the $[Ag_3L_2]^{3+}$ type cages are well-documented for many tripodal N-donor ligands,[15,16] formation of such a molecule in the present instance is driven by the relative reactivities of the Ag(I) salts. The ligand moieties in **2**·$3H_2O$ are C3-symmetric and resemble the "*Trie Cassyn*" symbol of the Isle of Man flag. While one of the ligands in a given $[Ag_3(LH_3)_2]^{3+}$ unit shows a clockwise rotation (Δ) of its pyridyl arms, that of the other one shows an anti-clockwise rotation (Λ) (Fig. 2b and c). Hence, each of the tri-cationic motifs in the crystal structure of **2**·$3H_2O$ is a racemate.

3·$5CH_3OH·3H_2O$ crystallized in the monoclinic space group *C*2/*c*. The molecular core is comprised of the tetra-cationic cluster of eight Ag(I) ions, which are held together by four anionic (LH_2^-) ligands. The charge balance is restored by the presence of four perchlorate anions that are disordered over five positions. Each of the four anionic ligands of type *b* (Fig. 1) binds to four Ag(I) ions through one imido and three pyridyl nitrogens. All of the eight Ag(I) centres in **3**·$5CH_3OH·3H_2O$ are involved in a linear coordination, in which two of them, Ag1 and Ag2, are located inside the cluster core and bonded solely with the imido groups. Thus, Ag1 is bonded to N3 and N9 and Ag2 is bonded to N6 and N12, respectively. The remaining six Ag(I) ions are situated along the corners of the cluster, as two triangular units, and interact with the pyridyl nitrogens (Fig. 3a). While the average $Ag–N_{imino}$ distance in **3**·$5CH_3OH·3H_2O$ is 2.114(4) Å, the $Ag–N_{pyridyl}$ contacts are found between 2.152(5) and 2.220(5) Å. The $P–N_{imino}$ distances (av. 1.605(4) Å) are marginally shorter than the other $P–N_{amino}$ distances (av. 1.667(4) Å) indicating the delocalized nature of the anionic charge inside the cluster. There are three short Ag–Ag contacts *viz.*, Ag1–Ag5: 2.752(6), Ag1–Ag2: 2.908(6) and Ag2–Ag3: 2.764(6), connecting the two inner (Ag1 and Ag2) and two outer (Ag3 and Ag5) cations. The phosphoryl oxygens are intra-molecularly hydrogen bonded in a concerted manner to one of the amino protons of the adjacent imido phosphate ligands. The remaining amino groups are hydrogen bonded to either perchlorate anions or the solvated molecules (Fig. S6a, ESI†). Furthermore, the twelve pyridyl rings of the four (LH_2^-) ligands, situated along the cluster rims, form a set of four π–π stacked triads. Within a given triad the inter-ligand π–π interaction is stronger (av. 3.721(2) Å) than that of the intra-ligand (av. 4.098(2) Å) interaction (Fig. 3b). Formation of a 3D-supramolecular assembly was also observed as the outer Ag(I) centres form weak contacts with disordered perchlorates and solvent molecules (Fig. S6b, ESI†).

The crystal structure of **4**·H_2O was solved in the chiral hexagonal space group *R*3. The asymmetric unit consists of one third of the molecule where the ligand (LH^{2-}) and two Ag(I) ions (Ag1 and Ag2) take up the general positions. The third unique Ag(I) centre, labelled Ag3, the tetrafluoroborate anion and the water molecules sit at the three fold axis of symmetry and have one third occupancies each (Fig. 4a). Each of the three ligands in **4**·H_2O is bonded to five Ag(I) ions through its two imido (N1 and N2) and three pyridyl (N12, N22 and N32) nitrogens. Three different types of coordination are found for the Ag(I) ion in **4**·H_2O: an almost linear coordination for Ag1 (N1 and N12*), a tetra-coordination for Ag2 (N1, N2, N2** and N32) and a nearly planar tri-coordination for Ag3 (N22, N22* and N22**). While N1 forms the shorter (Ag1–N1: 2.140(7) Å) and the longer (Ag2–N1: 2.697(7) Å) contacts to Ag(I) ions, N2 interacts with two Ag2 ions at moderate distances (Ag2–N2: 2.286(7) Å and Ag2*–N2: 2.393(7) Å). The Ag–$N_{pyridyl}$ distances are similar to **2**·$3H_2O$ and **3**·$5CH_3OH$·$3H_2O$ and range from 2.139(8) Å (Ag1–N12) to 2.331(16) Å (Ag2–N32). It is worthwhile to note the arrangement of seven Ag(I) ions in **4**·H_2O, where the three crystallographically unique Ag centres are located in different layers. While the first and second layers contain the respective triangular arrays of Ag1 and Ag2 ions, Ag3 forms the third layer and serves as the capping unit (Fig. 4b). Thus, the structure of the cationic Ag_7 core can be viewed as a *mono-capped distorted prism*, in which the two triangular units of Ag1 and Ag2 deviate by an angle of 11.9°. The Ag–Ag distances in **4**·H_2O are found between 2.899(12) (Ag2–Ag3) and 3.219(13) (Ag1–Ag1*) Å and compares closely to those found in metallic silver (2.88 Å).[17] In the solid-state the molecules are arranged in the form of a 2D-hexagonal sheet through hydrogen bonding interactions (Fig. 4c). The cationic core consists of three Lewis-acidic NH sites that are bonded to three anionic BF_4 units through N–H···F H-bonding interactions. In addition, the water molecules, disordered over three sites, interact with the phosphoryl oxygens from the neighbouring clusters.

Although there are a number of reports pertaining to the structures of hepta- and octa-nuclear Ag(I) clusters,[18,19] most of them have been obtained in the presence of soft chalcogen (S or Se) or π-donor ligands. To the best of our knowledge, this is the first report on such hepta- and octa-nuclear complexes containing all nitrogen coordination. The observed mono- and di-deprotonation of the ligand protons in these complexes is driven by the relative reactivities of the Ag(I) salts, as well as the acidic nature of the amino protons in **1** indicated by its pK_a value of 4.01 in MeOH.[14] Further, the pyridyl rings of the ligands in **2**, **3** and **4** are arranged in a mutually *cis*-fashion and involved in encapsulating the cluster moieties. The P═O groups in all of these cases are pointing away from cluster centre and remain non-coordinating. Interestingly, related cyclic phosphazenes have shown a high affinity for silver(I), resulting in the formation of coordination polymers, which can accommodate up to five Ag(I) ions per ligand.[20]

In one of the crystallization reactions involving **1** and AgOAc, we observed the formation of a toluene adduct of **1** (**1**·C_7H_8), instead of the expected Ag(I) complex. This is attributed to the solvent incompatibilities of **1** and AgOAc under the given reaction conditions, resulting in the crystallization of **1**·C_3H_8. The structure of **1**·C_7H_8 was obtained in monoclinic *P*2(1)/*c* space group. The asymmetric unit consists of four molecules of $PO(NHpy)_3$ and four toluene molecules. The metric parameters associated with P–N and P═O bonds are comparable with the reported structures of **1**.[14,21] In the crystal structure of **1**·C_7H_8, two of the three amino protons in each ligand are inter-molecularly interacting with two pyridyl nitrogens forming a H-bonded dimer. These dimers are further connected through the phosphoryl oxygens and the remaining amino protons, leading to a chain structure (Fig. S7, ESI†). Interestingly, the packing diagram of it shows a 1D-channel structure in which solvated toluene molecules are occupied in the void space (Fig. 5).

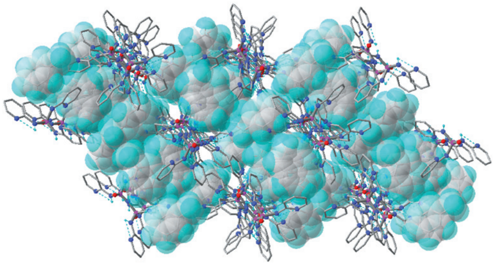

Fig. 5 Packing diagram of **1**·C_7H_8.

UV-visible and fluorescence spectra

The UV-visible spectra of the compounds **1**, **2**, **3** and **4** in DMSO show single absorptions arising from the pyridylamino chromophores and range between 282 nm (for **4**) and 285 nm (for **1**) (Fig. 6a). These values are found to be red shifted in the solid-state by about 50 nm (Fig. 6b) and range from 332 nm (for **1**) to 337 nm (for **4**), indicating that these transitions are predominantly n → π* in nature. The solution emission spectra of the ligand **1** and the complex **2** in DMSO show almost equal intensities and maxima at 325 nm. Similarly the emission maxima of **3** and **4** are nearly same at 328 and 330 nm, respectively, but show a quenching of fluorescence intensities by a factor of 50%. The solid-state fluorescence spectra of these compounds are again red shifted by about 50 nm confirming the n → π* transitions and ranges from 389 nm (for **1**) to 397 nm (for **4**) (Fig. 6d). Interestingly, as we move from the free ligand **1** to the Ag(I) complexes coordinated to neutral (**2**), mono-anionic (**3**) and di-anionic (**4**) ligands, the fluorescence intensities in the solid-state decrease progressively. Although such an effect can be expected in the solution emission spectra as well, the presumable dynamic nature of the Ag–N bonds in dilute solutions precludes such an observation. The calculated quantum yields of 0.065 (for **1**), 0.045 (for **2**), 0.020 (for **3**) and 0.018 (for **4**) in DMSO solutions are very low compared to the reference 2-aminopurine.

Conclusions

In summary, we have synthesized interesting examples of tri-, hepta- and octa-nuclear Ag(I) complexes starting from the 2-pyridyl-functionalized tris(amido) phosphate ligand. Utilizing the slight variations in the reactivities of the Ag(I) salts, sequential deprotonation of the ligand amino protons were achieved forming imido P(V) species analogous to the dihydrogen phosphate and mono hydrogen phosphate ions. The solid-state fluorescence spectra of the ligand and complexes show a sequential quenching of fluorescence intensities from the free ligand to the Ag(I) complex containing the di-anionic di-imido phosphate ligand. Such an observation has been made for the first time in imido-P(V) chemistry. Currently, work is in progress towards the mild synthesis of imido-phosphate tri-anions analogous to the PO_4^{3-} ion using various reactive metal salts.

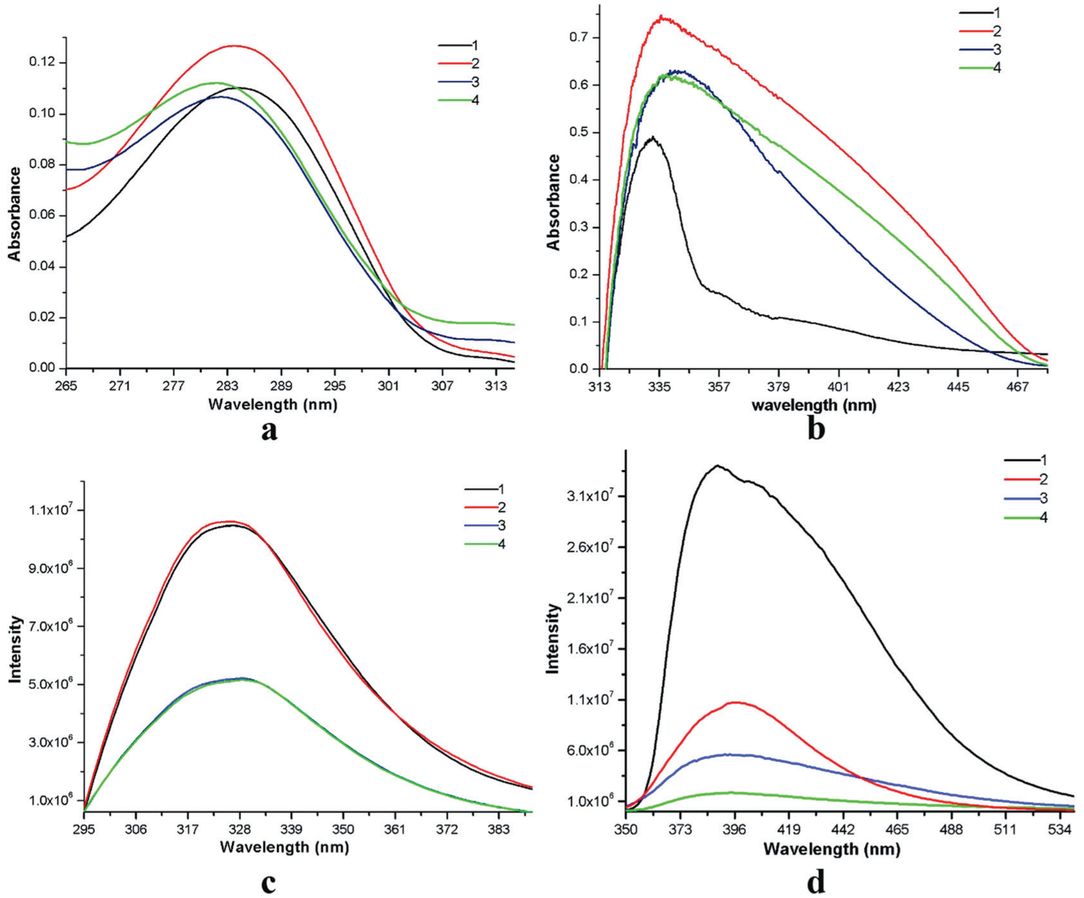

Fig. 6 UV-visible spectra of the compounds **1–4** (a) in DMSO solution and (b) in the solid-state. Fluorescence spectra of the compounds **1–4** (c) in DMSO solution (λ_{ex} = 327 nm) and (d) in the solid-state (λ_{ex} = 390 nm). All of the solution spectra were recorded at 10 μM concentration.

Experimental

General remarks

All manipulations involving phosphorus halides were performed under a dry nitrogen atmosphere in standard Schlenk glassware. Solvents were dried over potassium (hexane) and sodium (toluene). 2-aminopyridine and silver(I) salts were purchased from Aldrich and used as received. The halide precursor $POCl_3$ was purchased locally (SPECTROCHEM, India) and was distilled prior to use. NMR spectra were recorded on a Jeol 400 MHz spectrometer (^1H NMR: 400.13 MHz, $^{13}C\{^1H\}$NMR: 100.62 MHz, $^{31}P\{^1H\}$ NMR: 161.97 MHz) at room temperature using $SiMe_4$ (^1H, ^{13}C) and 85% H_3PO_4 (^{31}P) as external standards. The solid-state (CP-MAS) $^{31}P\{^1H\}$ NMR spectra were obtained on a Bruker 500 MHz spectrometer at a MAS rate of 10.0 KHz. The ESI-mass spectra in the positive ion mode were recorded in a Waters-SYNAPT-G2 high resolution spectrometer. UV-visible spectra were recorded by a Perkin-Elmer Lambda-35 spectrophotometer. The solid-state UV-visible spectra were obtained from Perkin-Elmer Lambda-950 UV-Visible NIR spectrophotometer with 150 mm integrating sphere. The emission spectra were obtained from Florolog-3 Horiba Jobin Vyon fluorescence spectrophotometer with a 450 W Xe lamp as the excitation source. Emission quantum yields were determined by comparison with the emission of a solution of 2-aminopurine (Φ_R = 0.68) in H_2O, employed as a standard.[22] The excitation wavelength used was 327 nm. The quantum yields were then calculated using the expression, $\Phi_S = \Phi_R(A_S/A_R)(n_S^2/n_R^2)$. The subscripts S and R denote sample and reference respectively. Φ is the fluorescence quantum yield, A is the integrated area under the corrected fluorescence spectra and n is the refractive index of the solvent. The solid-state emission spectra were obtained from the front face mode. Elemental analyses were performed on a Vario-EL cube elemental analyzer. FT-IR spectra were taken on a Perkin Elmer spectrophotometer with samples prepared as KBr pellets. Melting points were obtained using an Electro thermal melting point apparatus and were uncorrected.

Synthesis

$2{\cdot}3H_2O$. To a solution of **1** (100 mg, 0.306 mmol) in methanol (3 mL), containing a few drops of chloroform in a screw-capped vial, toluene (1 mL) was added followed by a careful layering of a solution of $AgNO_3$ (78 mg, 0.460 mmol) in water (3 mL). The resulting slightly cloudy solution was kept in the dark for crystallization. Colorless block-like crystals were obtained after 10 days. Yield 62% (113 mg, based on P). M. P. 180–182 °C, ^1H NMR(400 MHz, $\{(CD_3)_2SO\}$): δ 6.95 (s, CH),

Table 1 Crystallographic data[a]

Compound	**1**·C_7H_8	**2**·$3H_2O$	**3**·$5CH_3OH·3H_2O$	**4**·H_2O
Chemical formula	$C_{15}H_{15}N_6OP$	$C_{30}H_{36}Ag_3N_{15}O_{14}P_2$	$C_{65}H_{80}Ag_8Cl_4N_{24}O_{28}P_4$	$C_{45}H_{41}Ag_7BF_4N_{18}O_4P_3$
Formula weight	418.43	1216.29	2774.17	1832.77
Temperature	200(2)K	296(2)K	296(2)K	296(2)K
Crystal system	monoclinic	monoclinic	monoclinic	hexagonal
Space group	$P2_1/c$	$P2_1$	$C2/c$	$R3$
a (Å); α (°)	21.975(3); 90	14.0273(12); 90	49.075(3); 90	14.1261(3); 90
b (Å); β (°)	17.625(2); 130.373(6)	22.194(2); 98.846(5)	13.2864(7); 90.737(2)	14.1261(3); 90
c (Å); γ (°)	29.216(3); 90	14.8103(13); 90	27.6363(15); 90	24.5724(14); 120
V (Å^3); Z	8620.7(18); 16	4556.0(7); 4	18 018.2(17); 8	4246.4(3); 3
ρ (calc) mg m^{-3}	1.290	1.773	2.045	2.150
μ (Mo K$_\alpha$) mm^{-1}	0.154	1.422	1.981	2.528
$2\theta_{max}$ (°)	50	45	50	56
R(int)	0.1152	0.1091	0.0608	0.0527
Completeness to θ	99.5%	98.7%	99.4%	99.6%
Data/param.	15 154/1039	11 649/1004	15 842/903	4402/254
GOF	1.007	1.002	1.002	1.038
R_1 [$F > 4\sigma(F)$]	0.0537	0.0929	0.0438	0.0395
wR_2 (all data)	0.1414	0.2545	0.1121	0.1226
Flack parameter	—	0.58(6)	—	—
Max. peak/hole (e Å^{-3})	0.698/−0.437	1.911/−0.962	0.554/−0.686	1.181/−0.791

[a] Refer to the ESI† for the tables of bond-lengths and angles and H-bonding.

7.18 (br, C*H*), 7.72 (br, C*H*), 8.16 (br, C*H*), 8.96 (s, N*H*): ^{13}C {^1H}} (100 MHz, {$(CD_3)_2SO$}): δ 113.23, 117.12, 139.15, 148.56, 154.24: ^{31}P NMR (161 MHz, {$(CD_3)_2SO$}): δ −5.2; FT-IR data in KBr pellet (cm^{-1}): 3443, 3138 [ν (N–H)]; 510, 601, 629, 771, 824, 952, 994, 1053, 1098, 1154, 1207, 1242, 1295, 1384, 1445, 1487,1574, 1601 [ν (P–N)]; 1207, 1242 [ν (P═O)]; 647, 735 [ν (Ag–N)]. Anal. calcd for $C_{30}H_{30}N_{15}O_{11}P_2Ag_3$: C, 31.00; H, 2.60; N, 18.08. Found: C, 31.74; H, 2.58; N, 17.85.

3·5CH$_3$OH·3H$_2$O. To a solution of **1** (100 mg, 0.306 mmol) in methanol (2 mL) and chloroform (1 mL) in a screw-capped vial, toluene (1 mL) was added followed by a careful layering of a solution of $AgClO_4$ (127 mg, 0.612 mmol) in methanol (3 mL). The resulting slightly cloudy solution was kept in the dark for crystallization. Colorless block-like crystals were obtained after 3 days. Yield 72%, (149 mg, based on P). ^1H NMR(400 MHz, {$(CD_3)_2SO$}): δ 3.14 (s, C*H$_3$*), 6.97 (br, C*H*), 7.20 (br, C*H*), 7.74 (br, C*H*), 7.97 (br, C*H*), 8.24 (br, C*H*), 8.89 (s, N*H*): ^{13}C {^1H}} (100 MHz, {$(CD_3)_2SO$}): δ 113.51, 117.27, 139.36, 148.78, 154.23: ^{31}P NMR (161 MHz, {$(CD_3)_2SO$}): δ +1.5; FT-IR data in KBr pellet (cm^{-1}): 3416, 3126 [ν (N–H)]; 636, 724, 775, 958, 1061, 1293, 1418, 1449, 1488, 1598 [ν (P–N)]; 1228 [ν (P═O)]; 1025 [ν (Ag–N)]. Anal. calcd for $C_{60}H_{56}N_{24}O_{20}P_4Cl_4Ag_8$: C, 28.13; H, 2.20; N, 13.12. Found: C, 29.00; H, 2.74; N, 13.02.

4·H$_2$O. To a solution of **1** (100 mg, 0.306 mmol) in methanol and chloroform (3 mL) in a screw-capped vial, toluene (1 mL) was added followed by a careful layering of a solution of $AgBF_4$ (149 mg, 0.765 mmol) in methanol (3 mL). The resulting slightly cloudy solution was kept in the dark for crystallization. Light yellow colored single crystals were obtained in two weeks. Yield 60% (112 mg, based on P), M. P. 190–192 °C, ^1H NMR (400 MHz, {$(CD_3)_2SO$}): δ 6.88 (br, C*H*), 7.58 (br, C*H*), 8.16 (br, C*H*), 8.72 (br, C*H*), 8.87 (br, N*H*): ^{13}C {^1H}} (100 MHz, {$(CD_3)_2SO$}): δ 113.57, 115.26, 139.00, 148.69, 154.61: ^{31}P NMR (161 MHz, {$(CD_3)_2SO$}): δ +9.3; FT-IR data in KBr pellet (cm^{-1}): 3189 [ν (N–H)]; 690, 748, 956, 1031, 1081, 1280, 1410, 1498 [ν (P–N)]; 1221 [ν (P═O)]; 647, 736, 750 [ν (Ag–N)]: Anal. calcd for $C_{45}H_{39}BN_{18}O_3F_4P_3Ag_7$: C, 29.78; H, 2.17; N, 13.89. Found: C, 30.11; H, 2.58; N, 13.85.

1. C$_7$H$_8$. To a solution of **1** (100 mg, 0.306 mmol) in methanol (3 mL), containing a few drops of chloroform in a screw-capped vial, toluene (1 mL) was added followed by a careful layering of a solution of AgOAc (153 mg, 0.916 mmol) in water (3 mL). The resulting slightly cloudy solution was kept in the dark for crystallization, from which colorless block-like crystals of **1** formed. C_7H_8 was obtained after 10 days. The analytical and spectroscopic data of the sample dried at 60 °C under vacuum matches with the reported values of **1**.

Crystallography

Reflections were collected on a Bruker Smart Apex II diffractometer at 296 K using MoK$_\alpha$ radiation (λ = 0.71073 Å) for **2**·$3H_2O$, **3**·$5CH_3OH·3H_2O$ and **4**·H_2O. The data for **1**·C_7H_8 were collected on Bruker Smart Apex Duo diffractometer at 200 K using MoK$_\alpha$ radiation (λ = 0.71073 Å). Structures were refined by full-matrix least-squares against F^2 using all data (SHELX).[23] Crystallographic data for **1**·C_7H_8, **2**·$3H_2O$, **3**.$5CH_3OH·3H_2O$ and **4**·H_2O are listed in Table 1. All non-hydrogen atoms were refined anisotropically, if not stated otherwise. Hydrogen atoms were constrained in geometric positions to their parent atoms. One of the toluene molecules in **1**·C_7H_8 was disordered and was refined isotropically over two sites. Crystals of **2**·$3H_2O$ were slightly opaque and diffracted only weakly lacking observed reflections at higher angles and hence a 2θ cut-off at 45° was applied. Although the overall connectivity is not in doubt, care should be taken when evaluating bond lengths and angles. Due to the poor quality of data, atom positions of the nitrate and water moieties were refined isotropically. The nitrate ions were refined with similar-distance restraints and global similar-U restraints were applied to all C, N and O atoms. The structure of **2**·$3H_2O$ was refined as a racemic twin. In **3**·$5CH_3OH$·$3H_2O$ the perchlorate anions and solvent molecules are severely disordered along channels that run between the cationic complexes. NMR data suggest that there are about 5 methanol and 3 water molecules per formula unit. The perchlorate ions and solvent molecules were treated as a diffuse contribution to the overall scattering without specific atom positions by SQUEEZE/PLATON. In addition, we also provide a model that attempts to describe the disorder. Isotropic refinement with tight restraints gave tetrahedral ClO_4^- ions, albeit with large thermal parameters; electron difference peaks due to solvents where refined as partially occupied oxygen atoms. In **4**·H_2O one pyridyl group is disordered. It was split over two positions and refined isotropically with occupancy factors and similar distance and similar U restraints. Both the BF_4^- anion and the lattice water molecule are disordered over the 3-fold axis. The BF_4^- anion was refined isotropically with similar distance and similar U-restraints.

Acknowledgements

This work was supported by the Department of Science and Technology, India through Grant No. SR/FT/CS-014/2008 (R. B.) and IISER, Pune. We thank Dr T. S. Mahesh for providing help in obtaining solid-state NMR spectra.

Notes and references

1 (*a*) T. Chivers and J. K. Brask, *Angew. Chem., Int. Ed.*, 2001, **40**, 3960; (*b*) M. A. Beswick, M. E. G. Mosquera and D. S. Wright, *J. Chem. Soc., Dalton Trans.*, 1998, 2437; (*c*) D. S. Wright, *Coord. Chem. Rev.*, 1998, **176**, 373; (*d*) R. Fleischer and D. Stalke, *Coord. Chem. Rev.*, 1998, **176**, 431; (*e*) M. Witt and H. W. Roesky, *Chem. Rev.*, 1994, **94**, 1163.

2 (*a*) F. T. Edelmann, *Coord. Chem. Rev.*, 1994, **137**, 403; (*b*) P. J. Bailey and S. Pace, *Coord. Chem. Rev.*, 2001, **214**, 91; (*c*) G. M. Aspinall, M. C. Copsey, A. P. Leedham and C. A. Russell, *Coord. Chem. Rev.*, 2002, **227**, 217; (*d*) L. Stahl, *Coord. Chem. Rev.*, 2002, **210**, 203.

3 (*a*) A. Steiner, S. Zacchini and P. I. Richards, *Coord. Chem. Rev.*, 2002, **227**, 193; (*b*) P. R. Raithby, C. A. Russell, A. Steiner and D. S. Wright, *Angew. Chem., Int. Ed. Engl.*, 1997, **36**, 649; (*c*) L. T. Burke, E. H. Freire, R. Holland, J. C. Jeffery, A. P. Leedham, C. A. Russell, A. Steiner and A. Zagorski, *Chem. Commun.*, 2000, 1769.

4 J. F. Bickley, M. C. Copsey, J. C. Jeffery, A. P. Leedham, C. A. Russell, D. Stalke, A. Steiner, T. Stey and S. Zacchini, *Dalton Trans.*, 2004, 989.

5 (*a*) A. Armstrong, T. Chivers, M. Krahn, M. Parvez and G. Schatte, *Chem. Commun.*, 2002, 2332; (*b*) S. D. Robertson, T. Chivers and J. Konu, *J. Organomet. Chem.*, 2007, **692**, 4327; (*c*) A. Armstrong, T. Chivers, M. Krahn and M. Parvez, *Can. J. Chem.*, 2005, **83**, 1768.

6 (*a*) T. Chivers, M. Krahn, M. Parvez and G. Schatte, *Chem. Commun.*, 2001, 1922; (*b*) T. Chivers, M. Krahn, G. Schatte and M. Parvez, *Inorg. Chem.*, 2003, **43**, 3994; (*c*) A. Armstrong, T. Chivers, M. Parvez, G. Schatte and R. T. Boeré, *Inorg. Chem.*, 2004, **44**, 3453.

7 A. Armstrong, T. Chivers, M. Parvez and R. T. Boeré, *Angew. Chem., Int. Ed.*, 2004, **43**, 502.

8 (*a*) A. Buchard, A. Auffrant, C. Klemps, L. Vu-Do, L. Boubekeur, X. F. Le Goff and P. Le Floch, *Chem. Commun.*, 2007, 1502; (*b*) M. Sauthier, J. Fornié-Cámer, L. Toupet and R. Réau, *Organometallics*, 2000, **19**, 553.

9 (*a*) C. Zhang, W.-H. Sun and Z.-X. Wang, *Eur. J. Inorg. Chem.*, 2006, 4895; (*b*) J. D. Masuda, P. Wei and D. W. Stephan, *Dalton Trans.*, 2003, 3500; (*c*) O. Alhomaidan, C. Beddie, G. Bai and D. W. Stephan, *Dalton Trans.*, 2009, 1991; (*d*) K. Yadav, J. S. J. McCahill, G. Bai and D. W. Stephan, *Dalton Trans.*, 2009, 1636; (*e*) L. LePichon, D. W. Stephan, X. Gao and Q. Wang, *Organometallics*, 2002, **21**, 1362; (*f*) O. Alhomaidan, G. Bai and D. W. Stephan, *Organometallics*, 2008, **27**, 6343; (*g*) D. Li, S. Li, D. Cui, X. Zhang and A. A. Trifonov, *Dalton Trans.*, 2010, **40**, 2151.

10 (*a*) A. Buchard, R. H. Platel, A. Auffrant, X. F. Le Goff, P. Le Floch and C. K. Williams, *Organometallics*, 2010, **29**, 2892; (*b*) H. Sun, J. S. Ritch and P. G. Hayes, *Inorg. Chem.*, 2011, **50**, 8063; (*c*) M. T. Gamer, M. Rastätter, P. W. Roesky, A. Steffens and M. Glanz, *Chem.–Eur. J.*, 2005, **11**, 3165; (*d*) M. Rastätter, A. Zulys and P. W. Roesky, *Chem. Commun.*, 2006, 874; (*e*) M. T. Gamer, P. W. Roesky, I. Palard, M. Le Hellaye and S. M. Guillaume, *Organometallics*, 2007, **26**, 651; (*f*) B. J. Ireland, C. A. Wheaton and P. G. Hayes, *Organometallics*, 2010, **29**, 1079.

11 (*a*) M. Rastätter, A. Zulys and P. W. Roesky, *Chem.–Eur. J.*, 2007, **13**, 3606; (*b*) M. Rastätter, A. Zulys and P. W. Roesky, *Chem. Commun.*, 2006, 874; (*c*) T. K. Panda, A. Zulys, M. T. Gamer and P. W. Roesky, *Organometallics*, 2005, **24**, 2197.

12 (*a*) A. Buchard, H. Heuclin, A. Auffrant, X. F. Le Goff and P. Le Floch, *Dalton Trans.*, 2009, 1659; (*b*) V. Cadierno, J. Díez, J. García-Álvarez and J. Gimeno, *Organometallics*, 2005, **24**, 2801; (*c*) L. Boubekeur, S. Ulmer, L. Ricard, N. Mézailles and P. Le Floch, *Organometallics*, 2006, **25**, 315.

13 (*a*) A. K. Gupta, J. Nicholls, S. Debnath, I. Rosbottom, A. Steiner and R. Boomishankar, *Cryst. Growth Des.*, 2011, **11**, 555; (*b*) A. K. Gupta, A. Kalita and R. Boomishankar, *Inorg. Chim. Acta*, 2011, **372**, 152.

14 A. K. Gupta, F. A. S. Chipem and R. Boomishankar, *Dalton Trans.*, 2012, **41**, 1848.

15 (*a*) J. J. Henkelis, T. K. Ronson, L. P. Harding and M. J. Hardie, *Chem. Commun*, 2011, **47**, 6560; (*b*) Y.-Q. Huang, Z.-L. Shen, T.-a. Okamura, Y. Wang, X.-F. Wang, W.-Y. Sun, J.-Q. Yu and N. Ueyama, *Dalton Trans.*, 2008, 204; (*c*) J. Fan, W.-Y. Sun, T.-a. Okamura, J. Xia, W.-X. Tang and N. Ueyama, *New J. Chem.*, 2002, **26**, 199.

16 (*a*) E. R. Humphrey, N. C. Harden, L. H. Rees, J. C. Jeffery, J. A. McCleverty and M. D. Ward, *J. Chem. Soc., Dalton Trans.*, 1998, 3353; (*b*) H.-K. Liu, X. Huang, T. Lu, X. Wang, W.-Y. Sun and B.-S. Kang, *Dalton Trans.*, 2008, 3178; (*c*) W.-Y. Sun, J. Fan, T.-a. Okamura, J. Xie, K.-B. Yu and N. Ueyama, *Chem.–Eur. J.*, 2001, **7**, 2557.

17 N. N. Greenwood and A. Earnshaw, *Chemistry of the Elements*, Pergamon Press, New York, 1989, p. 1368.

18 (*a*) C. W. Liu, I.-J. Shang, J.-C. Wang and T.-C. Keng, *Chem. Commun.*, 1999, 995; (*b*) K. Tang, X. Jin, H. Yan, X. Xie, C. Liu and Q. Gong, *J. Chem. Soc., Dalton Trans.*, 2001, 1374; (*c*) C. W. Liu, C.-M. Hung, H.-C. Haia, B.-J. Liaw, L.-S. Liou, Y.-F. Tsai and J.-C. Wang, *Chem. Commun.*, 2003, 976; (*d*) C. W. Liu, H.-W. Chang, C.-S. Fang, B. Sarkar and J.-C. Wang, *Chem. Commun.*, 2010, **46**, 4571; (*e*) E. Block, M. Gernon, H. Kang, G. Ofori-Okai and J. Zubieta, *Inorg. Chem.*, 1989, **28**, 1263; (*f*) I. G. Dance, L. J. Fitzpatrick, D. C. Craig and M. L. Scudder, *Inorg. Chem.*, 1989, **28**, 1853; (*g*) J. Vicente, P. González-Herrero, Y. García-Sánchez and P. G. Jones, *Inorg. Chem.*, 2009, **48**, 2060; (*h*) C. W. Liu, H.-W. Chang, B. Sarkar, J.-Y. Saillard, S. Kahlal and Y.-Y. Wu, *Inorg. Chem.*, 2010, **49**, 468.

19 (*a*) Q.-M. Wang and T. C. W. Mak, *Angew. Chem., Int. Ed.*, 2001, **40**, 1130; (*b*) H.-B. Wu, Z.-J. Huang and Q.-M. Wang, *Chem.–Eur. J.*, 2010, **16**, 12321; (*c*) X.-L. Zhao, Q.-M. Wang and T. C. W. Mak, *Inorg. Chem.*, 2003, **42**, 7872; (*d*) Q.-H. Wei, L.-Y. Zhang, G.-Q. Yin, L.-X. Shi and Z.-N. Chen, *J. Am. Chem. Soc.*, 2004, **126**, 9940; (*e*) K. Matsumoto, R. Tanaka, R. Shimomura and Y. Nakao, *Inorg. Chim. Acta*, 2000, **304**, 293; (*f*) X.-L. Zhao and T. C. W. Mak, *Polyhedron*, 2006, **25**, 975.

20 (*a*) P. I. Richards, J. F. Bickley, R. Boomishankar and A. Steiner, *Chem. Commun.*, 2008, 1656; (*b*) P. I. Richards and A. Steiner, *Inorg. Chem.*, 2004, **43**, 2810.

21 K. Gholivand, M. D. Alavi and M. Pourayoubi, *Z. Kristallogr.*, 2004, **219**, 124.

22 I. B. Berlman, *Handbook of Fluorescence Spectra of Aromatic Molecules*, Academic Press, New York, 1965.

23 G. M. Sheldrick, *Acta Crystallogr., Sect. A: Fundam. Crystallogr.*, 2008, **A64**, 112.